Polymer Chemistry

Accepted Manuscript

This is an *Accepted Manuscript*, which has been through the Royal Society of Chemistry peer review process and has been accepted for publication.

Accepted Manuscripts are published online shortly after acceptance, before technical editing, formatting and proof reading. Using this free service, authors can make their results available to the community, in citable form, before we publish the edited article. We will replace this *Accepted Manuscript* with the edited and formatted *Advance Article* as soon as it is available.

You can find more information about *Accepted Manuscripts* in the Information for Authors.

Please note that technical editing may introduce minor changes to the text and/or graphics, which may alter content. The journal's standard Terms & Conditions and the Ethical guidelines still apply. In no event shall the Royal Society of Chemistry be held responsible for any errors or omissions in this *Accepted Manuscript* or any consequences arising from the use of any information it contains.

ROYAL SOCIETY OF CHEMISTRY

www.rsc.org/polymers

Polymer Chemistry

ARTICLE

Studies on Homologous Random and Alternating Segmented Conjugated Polymers with and without Silicon Synthesized by ADMET

Received 00th January 20xx,
Accepted 00th January 20xx

DOI: 10.1039/x0xx00000x

www.rsc.org/

Gagandeep Singh,[a,b] Hamid Ardolic[a] and Ralf M. Peetz[a,b]

Using acyclic diene metathesis (ADMET), we synthesized homologous luminescent conjugated polymers with two aromatic segments based on thiophene and substituted phenylene, either alternating or randomly distributed, either directly connected or separated by Si-linkers. In the polymers with Mn ~5000 – 14600 g/mol, random or alternating placement of two segments yielded similar electro-optical properties (absorption λ_{max} at ~363 nm, emission λ_{max} ~411 nm, HOMO-LUMO gap 3.00-3.07 eV), although alternating segments showed a slightly more defined absorption with slightly higher absorptivity and emission efficiency (57% vs. 51%). Alternating segments directly conjugated (without a Si-linkers) showed longer wavelength absorption and emission (λ_{max} at ~490 nm and ~556 nm respectively), and slightly lower emission efficiencies (40%), as well as a smaller HOMO-LUMO gap of 2.21 eV. DFT calculations support the above results and analyses. Understanding such specific interactions between the aromatic units might provide guidance for future designs of segmented conjugated polymers.

Dedicated to Prof. Dr. Hermann Matschiner

Introduction

The developments of next generation light weight, flexible and printed electronics have revolutionized the field of conjugated polymers.[1] Consequently, a multitude of conjugated polymeric materials have been reported and incorporated into organic photovoltaics (OPVs), organic field-effect transistors (OFETs), organic light-emitting diodes (OLEDs), other applications.[2-7] The class of Si-containing conjugated polymers have received particular attention as conductors, semiconductors, light emitters, light harvesters in photoelectrics and photovoltaic systems.[8-21] The photophysical properties of such materials can be tailored by careful selection of electro-optically active conjugated aromatic segments, particularly in the polymer backbone.[22] The uniqueness of silicon containing segmented conjugated polymers is due to the discrete size and structure of said aromatic segments with well-defined electro-optical properties, compared to polymeric analogues with average distributions of conjugated segments.[23,24] While the conjugated segments electronically interact through space, due to their vicinity to each other, the polymers may also feature σ-π conjugation between the σ orbitals of the silicon atoms and π orbitals of the organic segment in the polymer chain.[24] Along with the electronic effects, silylene spacers, especially dialkylsilylenes, have also been shown to introduce significant flexibility into the polymeric chain, making such otherwise typically rigid-rod like polymers soluble and processable.[14, 25-29] Furthermore, intramolecular energy transfer from photoexcited states reported for organosilicon polymers may present alternatives donor-acceptor systems.[23, 26, 30]

The most common techniques to access conjugated polymer systems containing silicon are condensation-based syntheses[10, 11, 31] and hydrosilylation techniques.[24, 30, 32-42] We and others have reported using acyclic diene metathesis (ADMET) as a convenient route to precise polymer architectures that would not be accessible by any other methods, including silicon containing systems.[23, 43-49] Such control over polymer architecture is highly beneficial for varying material properties and determining potential applications.[46] Various functional groups can be incorporated into the polymer backbone owing to the reactivities of catalysts developed by Grubbs, Schrock, and Hoveyda.

In 2008, we reported ADMET as a convenient route to yield silylene- and siloxane-containing conjugated polymers and

[a] City University of New York, Graduate Center and College of Staten Island, 2800 Victory Boulevard, NY-10314, USA. Email: Ralf.peetz@csi.cuny.edu
[b] Ph.D. Program in Chemistry, The Graduate Center of the City University of New York, New York, NY 10016, USA

Electronic Supplementary Information (ESI) available: [^{13}C NMR spectra and 2D correlation data for polymers, TGA, DSC, more DFT calculation details of synthesized materials, additional synthetic details]. See DOI: 10.1039/x0xx00000x

macrocycles featuring alternating aromatic and silicon segments.[23] The resulting polymers emitted at wavelengths in the blue region with quantum efficiencies ~0.24-0.28. Later, we used ADMET for the controlled synthesis of fluorescent macrocycles consisting of aromatic segments linked by germanium containing segments.[47] Interrante et al. reported on using a related ADMET approach for the synthesis of photocurable, photoluminescent polycarbosilanes.[28] Recently, we reported on conjugated homo- and co-polymers containing both silicon and tri- or tetra-coordinated boron in the main chain. These polymers exhibited intriguing electro-optical properties. E.g., the copolymer with tri-coordinated boron served as a highly sensitive Lewis-donor sensor, as demonstrated by very efficient fluorescence quenching by fluoride ion binding.[44]

We hereby report the extension of the ADMET strategy to synthesize structurally related segmented conjugated polymers that feature two different electro-optically active aromatic segments, linked by a flexible silylene group or connected directly to each other. The segments in the silylene-containing systems were either distributed randomly along the chain or strictly alternating. The aromatic segments were based on thiophene and diheptyloxy substituted phenylene. To this end, three distinct bis-vinyl functional monomers were synthesized and subjected to ADMET polycondensation. The Si-containing systems were found to be emitting at blue wavelengths, whereas homologous systems without Si-linkages emitted at longer wavelengths. Blue-light-emitting polymers are of significant interest as energy transfer host materials in the presence of lower energy fluorophores.[9] Furthermore, the synthesized polymers were observed to exhibit energy transfer from one segment to another. Such intramolecular energy transfers along macromolecular organosilicon systems have received attention as they may serve as a useful model to mimic the natural light harvesting process.[26, 30, 42] The observations could be explained using results from electrochemical measurements and theoretical calculations of the HOMO/LUMO levels.

Experimental

General Information

All experiments involving air/moisture sensitive materials were carried out using standard Schlenk techniques with a dry nitrogen - filled dual manifold (inert gas/ vacuum).

Materials

5-Bromo-2-thiophenecarboxaldehyde (98%), n-butyllithium solution (BuLi, 2.5 M in hexane), methyltriphenylphosphonium bromide (98%), dichlorodimethylsilane (>99.5%), Grubbs' catalyst (2nd Generation), Hoveyda-Grubbs catalyst (2nd Generation), and diethyl ether (anhydrous) were obtained from Sigma-Aldrich. 1-bromo-2,5-bis(heptyloxy)-4-vinylbenzene and 2-bromo-5-vinylthiophene were prepared according to previous work.[67] Column chromatography was carried out on silica gel 60 (70-230 or 230-400 mesh) from EMD Chemicals. Solvents such as tetrahydrofuran (THF), toluene, hexane, and dichloromethane were purchased as HPLC grade from Fisher Scientific. Solvents were dried and degassed by a "Pure Solv" solvent purification system (using activated alumina, copper catalyst, molecular sieves column) by Innovative Technology Inc. before use. Deuterated solvents for NMR spectroscopy were from Cambridge Isotope laboratories.

Analytical Methods

600 MHz ^{1}H-NMR, 125 MHz ^{13}C NMR spectra, and 120 MHz ^{29}Si NMR were recorded in $CDCl_3$ on Varian Unity NMR instruments. All signals in the ^{1}H NMR spectra are reported in ppm relative to the solvent's residual ^{1}H signal ($CDCl_3$: 7.24 ppm) and with multiplicity (s = singlet, d = doublet, t = triplet, q = quadruplet, m = multiplet, dd = doublet of doublet). ^{13}C NMR and ^{29}Si NMR spectra were referenced to $CDCl_3$ (77 ppm) and tetramethylsilane (TMS) respectively. Thermogravimetric analysis was carried out on a Hi-Res TGA 2950 thermogravimetric analyzer from TA Instruments using a platinum pan with a heating rate 10 °C /min under continuous nitrogen flow.

UV-Visible absorption spectroscopy was performed on Perkin Elmer Model 650 UV Spectrophotometer with 1-cm path length cells in hexane. Photoluminescence spectra were recorded using a Varian spectrofluorometer with 1-cm path length cells in hexane. Gel permeation chromatography (GPC) analysis in THF was performed on an Alliance GPCV 2000 (Waters) instrument equipped with four Waters Styragel HR columns, i.e. HR-1, HR-3, HR-4, and HR-5E. The flow rate of THF was kept at 1.0 mL/min at 40 °C throughout the analysis. Molecular weights are recorded relative to polydispersity polystyrene standards. Absolute molecular weight and structural studies were performed on Viskotek TDA max (Model 305) equipped with advanced temperature controlled, triple-detector GPC system with Refractive Index, Viscometer and Light scattering detectors. Cyclic voltammetry (CV) experiments were carried out on a CV-50W analyzer from BAS. The three electrode system consisted of an Au disk as working electrode, a Pt wire as secondary electrode and an Ag wire as the reference electrode. The voltammograms were recorded with ~ 10^{-3} - 10^{-4} M solutions in THF and 0.1 M $Bu_4N[PF_6]$ as supporting electrolyte. The scans were referenced to ferrocene as internal standard. The potentials are reported relative to the ferrocene/ferrocenium couple.

Calculations

Density functional theory calculations were carried out on dimer models of the polymers and diheptyloxy were replaced with methyloxy for the sake of simplicity of calculations. The input files were prepared via Gaussview 3.07. First, the geometries of the dimer models were optimized in the ground state using basis set DFT/B3LYP/6-31G(d,p) in Gaussian 09[50] with CUNY high performance computers. The calculations were carried out in gas phase to neglect the solvent effect.[51]

Synthesis of 1

1-bromo-2,5-bis(heptyloxy)-4-vinylbenzene (700 mg, 1.70 mmol) was dissolved in a mixture of 5.4 mL dry THF and 0.6 mL of dry diethyl ether. This first solution was cooled to -78 °C and n-BuLi (0.70 mL, 2.5 M in hexanes, 1.70 mmol) was added through a syringe. The mixture (solution 1) was stirred at -78 °C for 3 hours. Dicholorodimethlylsilane (0.20 mL, 1.70 mmol) dissolved in 1 mL THF (solution 2) and cooled to -78 °C. Solution 1 then was transferred via cannula to solution 2, and the resulting mixture stirred at -78 °C for 4 additional hours to

form a monochloro-substituted silane intermediate (solution 3). In a separate reaction tube, 2-bromo-5-vinylthiophene (322 mg, 1.70 mmol) in 5.4 mL dry THF and 0.6 mL dry diethyl ether was cooled to -78 °C, and then n-BuLi (0.70 mL, 2.5 M in hexanes, 1.70 mmol) was added via syringe. This mixture was stirred at -78 °C for 3 hours to form lithiated vinylthiophene (solution 4). Solution 3 was then transferred drop-wise via cannula to solution 4 and the resulting mixtures stirred at -78 °C for 2.5 hours to yield monomer **1**. The solvent was evaporated, and the dry mixture was dissolved in hexane/toluene (1:1). The mixture was washed with water. After evaporating the solvent, the crude product was purified using a 70-230 mesh size silica gel column using hexane/toluene (4:1) as an eluent. Monomer 1 was yielded as a light green viscous liquid (585 mg, 66%). ^{1}H NMR (600 MHz, $CDCl_3$): 7.14 (d, ^{3}J = 3.43 Hz, 1H), 7.07-7.02 (dd, ^{4}J = 11.40 Hz, ^{3}J = 18.00 Hz, 1H), 7.02 (d, ^{3}J = 3.24 Hz, 1H), 6.92 (s, 1H), 6.84-6.80 (dd, ^{4}J = 11.40 Hz, ^{3}J = 17.40 Hz, 1H), 6.83 (s, 1H), 5.74 (d, ^{3}J = 17.89 Hz, 1H), 5.57 (d, ^{3}J = 17.47 Hz, 1H), 5.26 (d, ^{3}J = 11.31 Hz, 1H), 5.12 (d, ^{3}J = 10.94 Hz, 1H), 3.92 (t, ^{3}J = 6.59 Hz, 2H), 3.85 (t, ^{3}J = 6.48 Hz, 2H), 1.77-1.24 (m, 20H), 0.89 (m, 6H), 0.59 (s, 6H). ^{13}C NMR (125 MHz, $CDCl_3$): 158.96, 151.11, 149.31, 139.08, 136.35, 132.87, 130.75, 130.31, 127.89, 126.83, 121.72, 115.46, 114.40, 108.62, 70.58, 69.15, 32.76, 30.39, 30.05, 27.04, 23.63, 15.10, 0.04. Elemental analysis: calculated C 72.23, H 9.30, S 6.43; found C 72.21, H 9.33, S 6.65.

Synthesis of [(E)-1,2-bis(5-bromothiophen-2-yl)ethene]

2-bromo 5-vinylthiophene (395 mg, 2.09 mmol) was dissolved in 10 mL dry toluene and Grubbs second generation catalyst (87 mg, 0.10 mmol) was added. The mixture was heated to 65 °C and stirred for 72 hours under reduced pressure at this temperature. The solvent was evaporated, and the crude product purified using column chromatography with silica gel. A bright yellow solid was yielded (260 mg, 71%). ^{1}H NMR (600 MHz, $CDCl_3$): 6.92 (d, ^{3}J = 3.62 Hz, 2H), 6.78 (s, 2H), 6.75 (d, ^{3}J = 3.64 Hz, 2H). Elemental analysis: calculated C 34.31, H 1.73, S 18.32; found C 35.15, H 1.95, S 18.16.

Synthesis of 2

1-bromo-2,5-bis(heptyloxy)-4-vinylbenzene (672 mg, 1.64 mmol) was dissolved in 5.4 mL dry THF and 0.6 mL dry diethyl ether. The solution was cooled to -78 °C and n-BuLi (654 µL, 2.5 M in hexanes, 1.64 mmol) was added via syringe. The mixture was stirred at -78 °C for 3 hours (solution 1). Dicholorodimethlylsilane (197 µL, 1.64 mmol) dissolved in 1 mL THF was cooled to -78 °C (solution 2). Solution 1 was then transferred via cannula to solution 2 at -78 °C. The mixture was stirred at -78 °C for four additional hours to form monochlorosubstituted methylsilane (solution 3). In separate reaction tube, to a solution of (E)-1,2-bis(5-bromothiophen-2-yl)ethene (286 mg, 0.82 mmol) dissolved in 5.4 mL dry THF and 0.6 mL dry diethyl ether, cooled to -78 °C, n-BuLi (654 µL, 2.5 M in hexanes, 1.64 mmol) was added via syringe. This mixture was stirred at -78 °C for 3 hours to form lithiated thiophene "dimer" (solution 4). Solution 3 was then added to solution 4 via cannula transfer and stirred at -78 °C for 3 hours and then allowed to warm up to room temperature overnight resulting in the formation of monomer 2. The reaction mixture was dried, dissolved in a minimum amount of chloroform and precipitated into methanol. It was then filtered and passed through silica gel column using hexane/toluene (4:1) as an eluent to yield monomer **2** as a light green, viscous liquid (475 mg, 60%). ^{1}H NMR (600 MHz, $CDCl_3$): 7.15 (d, ^{3}J = 3.13 Hz, 2H), 7.06 (s, 2H), 7.05 (d, ^{3}J = 3.10 Hz, 2H), 7.05-7.01 (dd, ^{4}J = 11.10 Hz, ^{3}J = 17.71 Hz, 2H), 6.92 (s, 2H), 6.83 (s, 2H), 5.72 (d, ^{3}J = 17.90 Hz, 2H), 5.25 (d, ^{3}J = 11.20 Hz, 2H), 3.92 (t, ^{3}J = 6.42 Hz, 4H), 3.84 (t, ^{3}J = 6.42 Hz, 4H), 1.76-1.23 (m, 40H), 0.87 (m, 12H), 0.58 (s, 12H). ^{13}C NMR (125 MHz, $CDCl_3$): 158.95, 151.16, 148.80, 139.17, 136.66, 132.86, 130.33, 128.13, 126.84, 122.57, 121.75, 115.49, 108.64, 70.57, 69.21, 32.79, 30.43, 30.08, 27.07, 23.63, 15.11, 0.06. Elemental analysis: calculated C 71.85, H 9.15, S 6.61; found C 71.58, H 9.17, S 6.57.

Synthesis of 3

(2-(2,5-bis(heptyloxy)-4-vinylphenyl)-4,4,5,5-tetramethyl-1,3,2 diox-aborolane) (320 mg, 0.70 mmol) was dissolved in 3 mL dry THF and ((E)-1,2-bis(5-bromothiophen-2-yl)ethane) dimer (110 mg, 0.32 mmol was added to it. Tetrakis(triphenylphosphine)palladium catalyst (20 mg, 4 mol%) was added to the reaction mixture followed by the addition of 0.35 ml 4M K_3PO_4 solution. The reaction mixture was purged with nitrogen and stirred at 55 °C for 24h under nitrogen. The solvent was evaporated, and the dry mixture was dissolved in dichloromethane and washed with brine solution. After evaporating the solvent, the crude product is passed through 230-400 mesh size silica gel column using hexane/toluene (2:1) as an eluent to obtain pure monomer **3** as an orange solid (170 mg, yield 61%). ^{1}H NMR (300 MHz, $CDCl_3$): 7.42 (d, ^{3}J = 3.64 Hz, 2H), 7.12 (s, 2H), 7.05 (s, 2H), 7.02 (s, 2H), 6.98 (d, ^{3}J = 3.50 Hz, 2H), 6.98-7.05 (dd, 2H), 5.74 (d, ^{3}J = 17.60 Hz, 2H), 5.26 (d, ^{3}J = 11.10 Hz, 2H), 4.06 (t, ^{3}J = 6.52 Hz, 4H), 3.97 (t, ^{3}J = 6.26 Hz, 4H), 1.91-1.78 (m, 8H), 1.54-1.23 (m, 32H), 0.87 (t, ^{3}J = 6.53 Hz, 12H. ^{13}C NMR (125 MHz, $CDCl_3$): 150.66, 149.53, 142.35, 138.50, 131.40, 126.72, 126.20, 126.68, 123.42, 121.26, 114.29, 122.21, 110.81, 69.68, 69.42, 31.85, 29.49, 29.12, 26.18, 26.16, 22.67, 14.14. MALDI-TOF (pos.) *m/z*: calcd. for $C_{54}H_{76}O_4S_2$ [M-H$^+$] 852.52 found 853.74.

Typical Synthesis of P1

Monomer **1** (200 mg, 0.40 mmol) was dissolved in 4 mL dry toluene and Grubbs' second generation catalyst (34 mg, 0.04 mmol) or Hoveyda-Grubbs second generation catalyst (25.4 mg, 0.04 mmol) was added. The mixture was heated to 70 °C and stirred for 72 hours at this temperature under reduced pressure. The solvent was evaporated and the crude product was dissolved in dichloromethane and passed through silica gel plug. After solvent evaporation, **P1** was obtained as a viscous, sticky green semi-solid (120 mg, 60%). ^{1}H NMR (600 MHz, $CDCl_3$): 7.44 (s), 7.32-7.25 (m), 7.17(s), 7.10(s), 7.06-7.04 (m), 6.93 (s), 6.84 (s), 3.94 (t), 3.87 (t), 1.84-1.12 (m), 0.86 (m), 0.59 (s). ^{13}C NMR (125 MHz, $CDCl_3$): 159.10, 151.41, 148.98, 138.93, 136.67, 129.54, 127.90, 127.47, 127.20, 123.41, 123.26, 122.11, 121.90, 70.72, 69.06, 32.55, 31.23, 30.12, 27.13, 23.59, 15.13, 0.05. ^{29}Si NMR (120 MHz, $CDCl_3$): -12.95. UV-Vis (hexane, 1.87 x 10^{-6} M): λ_{max} = 363 nm (ε = 49727); fluorescence (hexane, 1.87 x 10^{-8} M): λ_{max} = 410 nm, 432 nm; $\Phi = 0.51$ (λ_{exc} = 363 nm). M_n (polystyrene standards) = 3705 g/mol; M_w/M_n = 1.58.

Typical Synthesis of P2

To monomer **2** (160 mg, 0.170 mmol) dissolved in 2.5 mL dry toluene, Hoveyda-Grubbs second generation catalyst (11 mg, 0.017 mmol) or Grubbs' second generation catalyst (13 mg, 0.016 mmol) was added. The mixture was heated to 70 °C and stirred for 72 hours at this temperature under reduced pressure. The solvent was evaporated, the crude product was then re-dissolved in toluene and passed through silica gel plug

to yield polymer **P2** as viscous, sticky yellow semi-solid (105 mg, 65 %). ^{1}H NMR (600 MHz, $CDCl_3$): 7.44 (s, 2H), 7.15 (d, ^{3}J = 3.38 Hz, 2H), 7.06 (s, 2H), 7.05 (d, ^{3}J = 3.46 Hz, 2H), 7.04 (s, 2H), 6.85 (s, 2H), 3.95 (t, ^{3}J = 6.52 Hz, 4H), 3.86 (t, ^{3}J = 6.44 Hz, 4H), 1.78-1.21 (m, 40H), 0.85 (m, 12H), 0.58 (s, 12H). ^{13}C NMR (125 MHz, $CDCl_3$): 159.10, 151.40, 148.76, 139.20, 136.66, 130.80, 128.11, 126.50, 125.10, 122.57, 122.14, 108.44, 70.85, 69.11, 32.99, 30.53, 30.08, 27.17, 23.53, 15.21, 0.05. ^{29}Si NMR (120 MHz, $CDCl_3$): -12.95. UV-Vis (hexane, 1.27 x 10^{-6} M): λ_{max} = 363nm (ε = 57,454); fluorescence (hexane, 1.27 x 10^{-8} M): $\lambda_{,max}$ = 411 nm, 434 nm, $\Phi = 0.57$ (λ_{exc} = 363 nm). M_n (polystyrene standards) = 4330 g/mol; M_w/M_n = 1.42.

Typical Synthesis of P3

(170 mg, 0.20 mmol) of **3** was dissolved in 2.5 mL dry toluene and Grubbs' second generation catalyst (8.5 mg, 0.01 mmol) was added. The mixture was heated to 70 °C and stirred for 72 hours at this temperature under reduced pressure. The reaction mixture was brought to room temperature and 0.5 mL of ethyl vinyl ether was added and stirred for 0.5h. The resulting solution was precipitated into 100 mL cold methanol and filtered to obtain **P3** as reddish brown powder (120 mg, 70% yield). ^{1}H NMR (600 MHz, $CDCl_3$): 7.48 (s, 2H), 7.46 (d, ^{3}J = 3.71 Hz, 2H), 7.20 (s, 2H), 7.18 (s, 2H), 7.06 (s, 2H), 7.02 (d, ^{3}J = 3.98 Hz, 2H), 4.13 (t, ^{3}J = 5.78 Hz, 4H), 4.04 (t, ^{3}J = 6.37 Hz, 4H), 1.97-1.84 (m, 4 H), 1.59-1.46 (m, 4 H), 1.44-1.29 (m, 32 H), 0.89 (t, ^{3}J = 5.96 Hz, 12H. ^{13}C NMR (125 MHz, $CDCl_3$): 150.88, 149.69, 142.31, 138.58, 128.64, 127.23, 126.53, 125.96, 123.47, 121.21, 122.32, 110.56, 69.59, 69.42, 31.87, 29.51, 29.10, 26.20, 26.12, 22.63, 14.18. UV-Vis (dichloromethane, 5.87 x 10^{-6} M): λ_{max} = 490 nm (ε = 43541); fluorescence (dichloromethane, 5.87 x 10^{-7} M): $\lambda_{,max}$ = 556 nm, $\Phi = 0.40$ (λ_{exc} = 490 nm). M_n (polystyrene standards) = 3139 g/mol; M_w/M_n = 2.01

Results and Discussion

We were interested in using ADMET to synthesize segmented conjugated polymers that feature two conjugated aromatic segments. The segments were placed either in direct conjugation with each other or separated by silicon linkages, randomly distributed or strictly alternating (Scheme 1). The influence of structure on the opto-electronic properties was then investigated. Precise sequence control in copolymerizations enables control of many properties of the copolymers, including thermal, crystalline,[46, 52] and as in our case opto-electronic.[43,53-56] The aromatic segments chosen are based on thiophene and *para*-phenylenevinylene because of their ubiquitous use as functional materials in applications based on conducting polymers, e.g. light-emitting diodes, plastic solar cells, etc..[13, 57-62] We were specifically interested in the cooperative properties of the two conjugated segments. The inclusion of aliphatic chains in the polymer structure ensures solubility and thus access to higher molecular weights, as well as processability. ADMET has been shown to successfully polymerize a wide variety of divinyl functional monomers.[45] To that end we synthesized two systems in which the segments would be separated by silicon linkage, one in which the segments are statistically distributed over the macromolecule, and another in which the segments strictly alternate. A third, homologous system was designed, featuring strictly alternating segments but lacking the silicon linkages, thus allowing for effective electronic conjugation between the segments. The three macromolecular systems are each required specially designed monomers.

Monomer Design and Synthesis

Scheme 1 details the synthetic strategies for monomers **1**, **2** and **3**. A key intermediate in the syntheses of **1** and **2** consisted of a chloro-silane functional bis(heptyloxy)vinylbenzene (Si-IM). Si-IM was synthesized from 1-bromo-2,5-bis(heptyloxy)-4-vinylbenzene (see Supporting Information) by lithiating and subsequently coupling it with one equivalent of dichloro-dimethyl silane. To yield **1**, a lithiated vinylthiophene (IM1) was combined in a 1/1 molar ratio with Si-IM. To yield **2**, a dilithiated (E)-1,2-bis(5-bromothiophen-2-yl)ethene (IM2) was coupled with Si-IM using a 1/2 molar ratio. (E)-1,2-bis(5-bromothiophen-2-yl)ethene had been previously prepared by homo-coupling two bromovinylthiophenes using olefin metathesis. (E)-1,2- for the synthesis of **3**, i.e. by coupling it with a boronic ester made from the above mentioned, 1-bromo-2,5-bis(heptyloxy)-4-vinylbenzene.

The ^{1}H NMR spectra (Supporting Information) of **1-3** indicate the formation of distinctive vinyl functions. In 1, one vinyl group attached to the thiophene ring and the other to the benzene ring are marked by four doublet signals in the region of 5.12 - 5.74 ppm. In **2** and **3**, only one type of vinyl function is present respectively, resulting in two doublet resonances each, at 5.25 and 5.72 ppm in **2**, and at 5.26 and 5.74 ppm in **3** respectively. Structure, purity, and composition were further supported by ^{13}C NMR (see Supporting Information), liquid chromatography, mass spectrometry, and elemental analysis.

Polymer Chemistry

ARTICLE

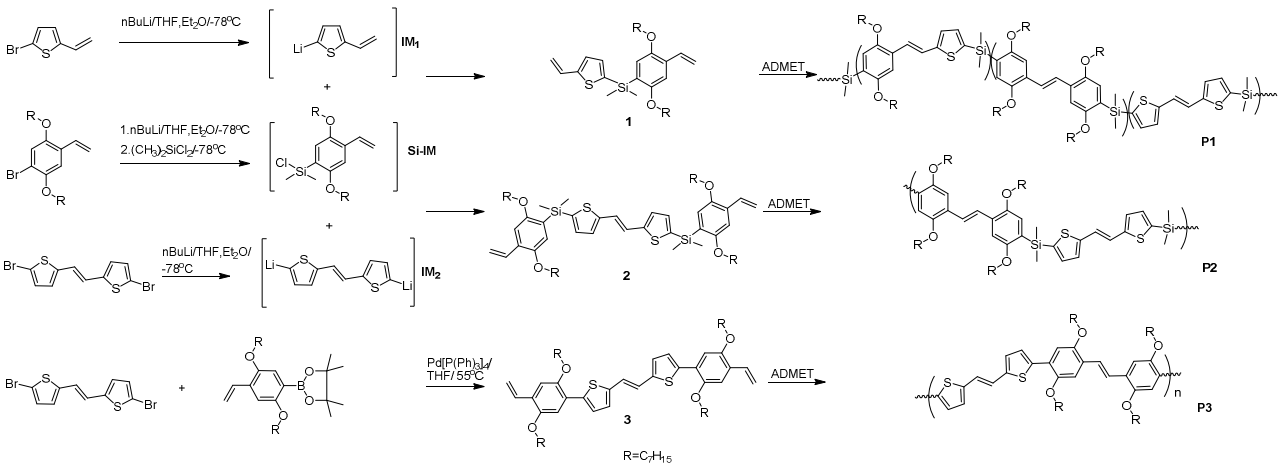

Scheme 1 Synthesis of monomers **1-3** and polymers **P1-P3**

Table 1 Representative ADMET polycondensations and polymer characteristics

	M (mol/L) [c]		Mn (g/mol)		PDI	T_d [d] (°C)	T_g (°C)
	[Monomer]	[Catalyst]	NMR	GPC			
P1 [a]	1.0×10^{-1}	1.0×10^{-2}	8829	3705	1.59	276/ 216	- 18
[b]			7888	3163	1.54		
P2 [a]	6.6×10^{-2}	6.6×10^{-3}	10713	3868	1.38	276/ 216	- 13
[b]			14589	4330	1.42		
P3 [a]	8.0×10^{-2}	8.0×10^{-3}	4982	3139	2.01	363/324	none [e]

[a] Grubbs 2nd generation catalyst; [b] Hoveyda – Grubbs 2nd generation catalyst; [c] t = 72h and T = 70 °C; [d] Decomposition temperature at 5% weight loss in N_2/O_2; [e] between -60 and 200 °C.

Polymerizations

Two catalysts were used for the ADMET polycondensations (Scheme 1), the ruthenium-based alkylidenes "Grubbs-Hoveyda second generation" [(1,3-bis(2,4,6-trimethylphenyl)-2-imidazolidinylidene) dichloro(*o*-isopropoxyphenyl-methylene)ruthenium] ($C_{31}H_{38}Cl_2N_2ORu$) and "Grubbs second generation" [1,3-bis(2,4,6-trimethylphenyl)-2-imidazolidinylidene) dichloro(phenyl methylene) (tricyclohexylphosphine) ruthenium] ($C_{46}H_{65}Cl_2N_2PRu$).[48, 63]

Optimizing the ADMET polycondensation of **1** involved varying reaction temperature, time, catalyst, catalyst concentration, as well as ratio catalyst/monomer. Typical reactions were carried out at 70 °C for the duration of 72 h under reduced pressure to shift the equilibrium towards the polymer by intermittent removal of ethylene gas.[64] Table 1 summarizes representative ADMET results for both catalysts. Under said conditions, and using [**1**]/[Catalyst]=1.0×10^{-1}M/1.0×10^{-2}M, M_n of 3705 and 3163 g/mol (GPC with PS standard, Supporting Information) were reached using Grubbs second generation and Grubbs-Hoveyda second generation catalysts respectively. Compared to the GPC results, NMR end group analysis generally indicated higher degrees of polymerization with respective Mn of 8829 and 7888 g/mol.

Earlier studies indicated significantly different conditions for the ADMET coupling of vinyl-functional thiophenes and benzenes.[67] This was not observed for the two different vinyl functions in **1**. Attempts to first selectively homo-couple the vinyl-thiophene side of **1** and then subsequently the vinyl-benzene function did not yield success. In fact, under all conditions investigated both vinyl functions seemed to have the same reactivity toward the catalyst systems at all stages of the reaction. As a result, the coupling was completely random as indicated by H-NMR analysis of **P1** vide infra).

In the case of **2**, Grubbs 2nd generation and Hoveyda – Grubbs 2nd generation catalysts yielded polymers **P2** with respective M_n of 3868 and 4330 g/mol per GPC (PS standards) (10,713 and 14,589 g/mol via H-NMR). **P3** was achieved using Grubbs 2nd Gen. catalyst with respective M_n of 3139 g/mol as per GPC (PS standards) (4982 g/mol with H-NMR end group analysis). The higher degrees of polymerization for **P1** and **P2** are most likely do to their higher solubilities due to the presence of flexible silylene linkages

The thermal stabilities of **P1** and **P2** are very similar. In N_2, 5% weight loss was observed at 276 °C whereas in O_2 this was reduced to 216 °C. Comparatively, **P3** is thermally more stable and exhibited 5% weight loss at 363 °C in N_2 and 324 °C in O_2. Differential scanning calorimetry (DSC) yielded glass transition temperatures for

P1 and **P2** at -18 °C and -13 °C respectively. T_g was not detected in DSC analysis of **P3** in the tested temperature range of -60 °C – 200 °C probably due to the rigid backbone of **P3** limiting chain mobility.[65]

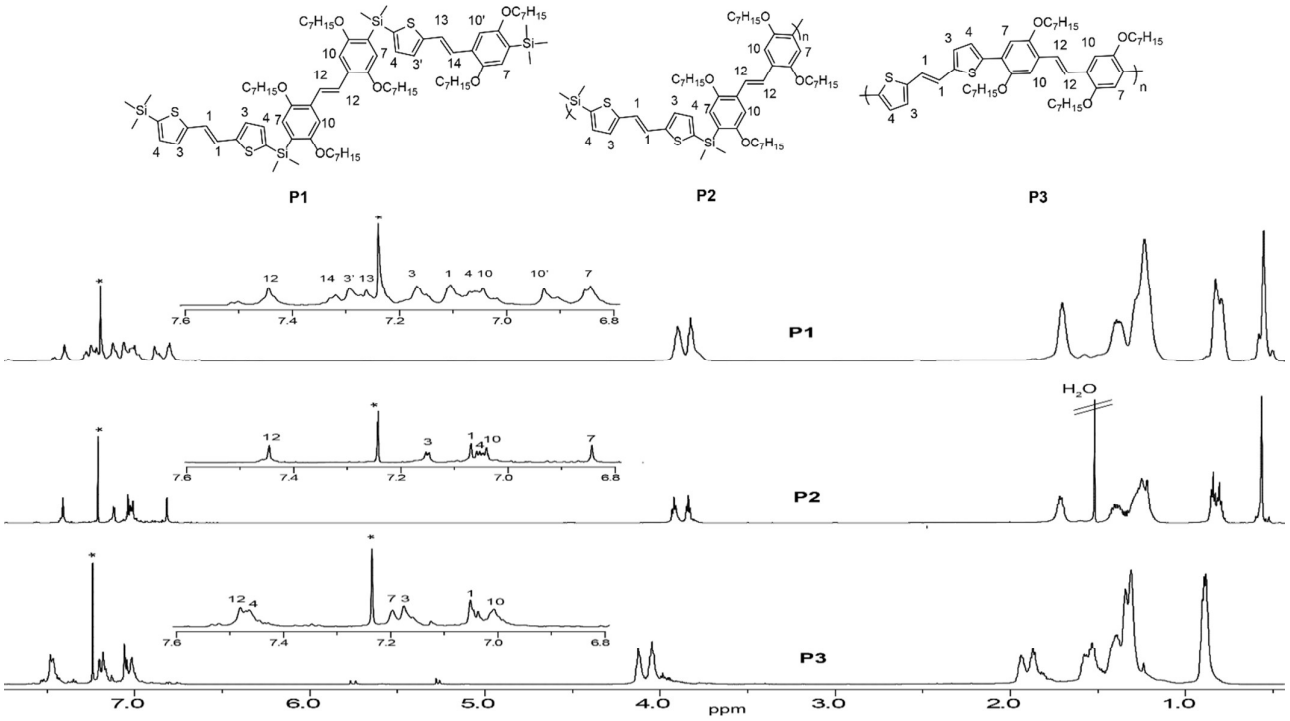

Figure 1 ^{1}H NMR spectra of **P1**, **P2** and **P3**

Microstructure of ADMET Polymers

Figure 1 shows ^{1}H-NMR spectra of **P1** – **P3** with relevant assignments. In **P1** three types of vinylene functions arise from the three possible coupling modes. Homo coupling between vinyl-thiophene functions yields vinylene assigned with 1. Homo coupling between vinyl-benzene functions yields vinylene assigned as 12. "Hetero" coupling between the two functions yields vinylene with two protons assigned as 13 and 14. These three vinylene types are part of three distinct aromatic segments present in the polymer chain. As a result, resonances from protons on the aromatic rings also depend on the type of segment they are part of, i.e. protons 3 vs. 3' and 10 vs. 10'. Integration of the relevant resonance signals with integrated signal intensities of 1 / 12/ (13+14) ~ 1/ 1/ 2 indicates statistical ADMET coupling. This ratio was independent of reaction time and temperature, indicating similar reactivities of the two different vinyl functions in **1** under the conditions used (also: vide supra).

To produce strictly alternating segmented blocks in the polymer chain, we designed monomers **2** and **3** which already contain the preformed thiophene segment. ADMET polycondensation yields the second aromatic, phenylene containing block. The spectra of the segmented polymers **P2** and **P3** are very similar to that of **P1** (Figure 1), e.g. when comparing vinylene proton resonances 1 and 12. But they lack the resonances from the mixed aromatic segment containing both a thiophene and a benzene part, i.e. the resonances of the vinylene protons 13 and 14. As mentioned above, ^{1}H NMR end group analysis of **P2** yielded molecular weights of 10,713 – 14,589 g/mol, indicating degrees of polymerization between 11 and 15.

The progress of the polycondensation can easily be monitored by following a select few ^{1}H NMR resonances: The signal intensity of the vinyl end groups decreases with increasing degree of polymerization, while the intensities from the newly formed vinylene groups increases, i.e. proton 12 in the case of **P2** and **P3** and 1,12,13, and 14 in the case of **P1**. Residual signal intensity at ~4.0 ppm in the spectra of **P2** and **P3** arises from methylene protons $-OCH_2-$ in the outermost hetptyloxy side chains next to unreacted vinyl end groups. Especially at longer chain lengths, in general the polycondensation equilibrium can be expected to show evidence of macrocyles as a result of "back biting", potentially rendering NMR end group analysis for size-determination inappropriate. To probe for the presence of cyclic polycondensates we performed Mark-Houwink analyses of the polymers (Supporting Information). We did not detect the presence of cyclic structures in the product distributions, therefore lending confidence to the NMR based calculations.

The structures of **P1**, **P2**, and **P3** are further confirmed by ^{13}C NMR (Supporting Information), most characteristically showing clearly the formation of the new vinylene functions. 2D NMR experiments (Supporting Information) helped to unequivocally
assign every C and H resonance to the structures discussed. ^{29}Si NMR analysis for both **P2** and **P1** (Supporting Information) showed a single resonance around -12.9 ppm for both systems, indicating both facts, that the chemical environments

at the Si are very similar in both systems, and that no side reactions occurred at the Si during polycondensation. Furthermore, the shift corresponds to earlier results on related system.[23]

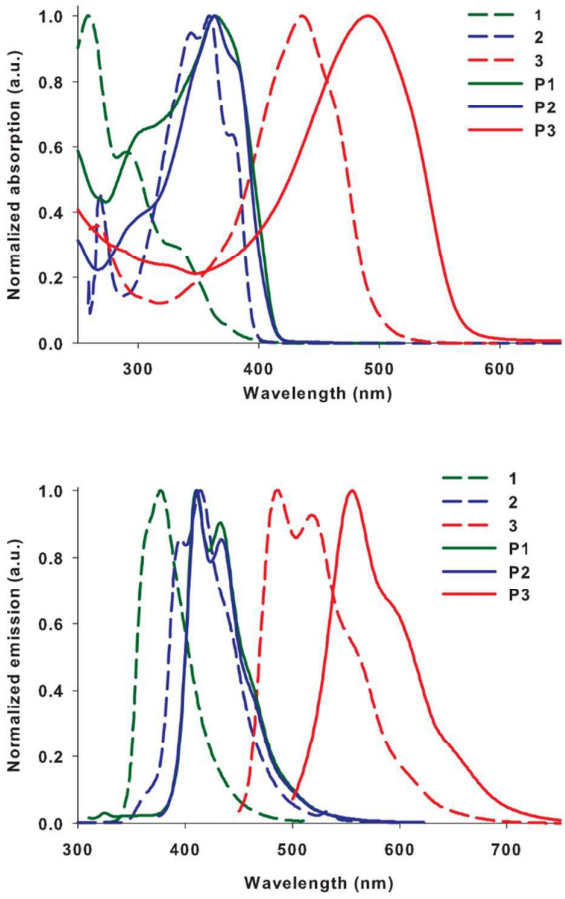

Figure 2 Absorption (top) and emission spectra (bottom) of **1-3** and **P1 – P3**

Optical properties

Figure 2 illustrates absorption and emission spectra of monomers and polymers. The measurements were performed using hexane solutions. In general, **P1** and **P2** absorbed in the UV and emitted in blue region. Earlier studies on optical properties of polymers containing trans-stilbene segments linked by silicon suggested that the Si linkages only allow for a weak electron delocalization between segments, thus resulting in polymer properties very similar to those of the isolated stilbene, albeit somewhat shifted to longer wavelengths, but still blue emission.[60]

1 showed three distinct absorptions at 259 nm, 292 nm and 336 nm. The absorption of **P1** is red shifted compared to **1** due to the aromatic segments with π – delocalization formed during ADMET. It showed a λ_{max} at ~ 363 nm with "shoulders" in the range of ~ 300 and 390 nm. Absorption of **2** showed a λ_{max} at ~ 359 nm with shoulders at ~ 344 and 377 nm, whereas P2 displayed a λ_{max} at ~ 363 nm with shoulders at ~ 300 and 382 nm. The red shift of the **P2** vs. **2** is not as strong as in case of **P1** vs. **1** because **2** already contains one of the two extended conjugated aromatic segments. **P2** and **P1** absorb at the same wavelength maximum, and very similar to **2**. However, the absorption of **P1** is broader and seems to contain more transitions than **P2** as evidenced in the line shape. This is to be expected as **P1** contains an additional type or extended conjugated aromatic segment not present in **P2**. Furthermore, the absorption seems to be dominated by the segment containing thiophene, as it is present in both polymer systems, as well as monomer **2**, leading to similar major absorptions. In comparison, the absorptions of **3** and **P3** are found at lower energies, i.e. at λ_{max} ~ 436 and 490 nm respectively. They lack the Si-linkage, thus enabling effective direct electron delocalization between the different aromatic segments of the monomer and then the polymer chain, resulting in a significant red shift.

The contribution of the stilbene-containing segment to the optical properties of **P1**, **P2**, and **2** is seen in the emission characteristics, as the emission maxima are observed at λ_{max} ~ 410, 411, and 414 nm respectively (with respective shoulders at ~ 432 and 434 nm for **P1** and **P2**). Another (weak) shoulder at ~470 nm is present regardless of concentration. **2** features an additional emission at ~ 394 nm and a weaker shoulder at ~ 440 nm. **1** is very different in its emission characteristics with λ_{max} ~ 376 nm and a shoulder at ~ 360 nm.The fact that **P1** with randomly distributed aromatic segments and **P2** with strictly alternating segments (and lacking the "mixed" segment containing both parts benzene and thiophene) show such similarities in absorption and emission is no coincidence. There are two potential explanations: (1) the excited state electronic interactions between thiophene and benzene units linked via internal vinylene bond are negligible, or (2) the emission process was quenched.

We compared the data of **P2** and **P1** with earlier results from polymers systems A and B (Scheme 2), each containing only one of the two aromatic segments found in **P2**, and connected similarly by a silylene linkage.[67,44] The absorption and emission spectra of A and B are overlayed with those of systems **P1** and **P2** in Figure 3. There is a significant overlap between the absorption of B and the emission of A. Also, the emission of **P2** closely resembles that of B, indicating the emission in **P2** (and in **P1**) is mainly emanating from the stilbene segment. This could be explained through possible fluorescence resonance energy transfer (FRET) from the thiophene containing segments in **P1** and **P2**, resulting also in a quenching of emission from these segments. This is supported by observations of FRET in earlier reports on silylene containing copolymers featuring alternating chromophores.[24, 26, 30, 33, 38] Fluorescence quantum efficiencies of **P1**, **P2**, and **P3** were determined as 0.51, 0.57, and 0.40 respectively (relative to trans-stilbene and anthracene). These values are significantly higher compared to related silicon-containing polymers having fluorophores such as phenylenevinylene, biphenylene and phenylene.[11, 23, 28] It appears that FRET from that bithiophenevinylene segment to the biphenylenevinylene segment is the reason for these higher quantum efficiencies.

As in the absorption, the emission of **P3** at λ_{max} ~ 556 nm is strongly red-shifted, compared to the other systems. Also, the emission characteristics cannot be associated with either of the two aromatic segments. The emission is the result of more extended conjugated electron systems, containing both segments. This conjugation is possible due to the absence of

the Si linkers. Table 2 summarizes the absorption and the emission results of the monomers and the polymers.

Table 2 Optical Properties of Monomers and Polymers

Sample	$\lambda_{max,ab}$ (nm)	$\lambda_{max,em}$ (nm)[1]	ϵ (L mol^{-1} cm^{-1})	Φ_{eff}
1	259, 292, 335	376	-	-
2	344,359	394, 414	-	-
3	436	485, 517	-	-
P1	363	410, 432	49727	0.51
P2	363	411, 434	57454	0.57
P3	490	556	43541	0.40

[1]excited at absorption maximum

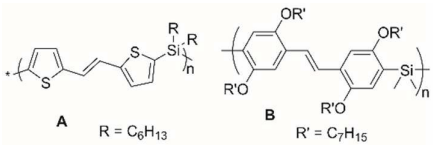

Scheme 2 Model polymers A, B

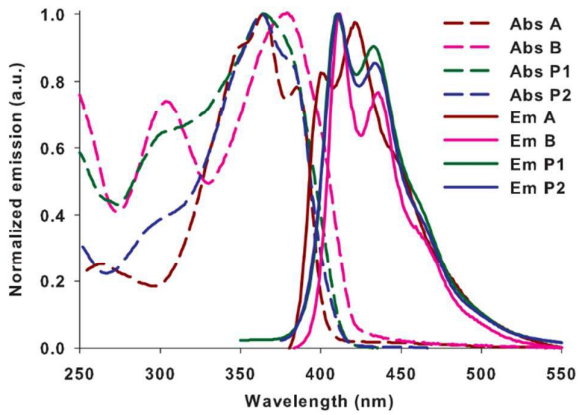

Figure 3 Absorption (Abs) and emission (Em) of **A**, **B**, **p1** and **p2**

but a lower energy LUMO compared to systems **P1** and **P2**, thus lowering the band gap from ~ 3.0 eV to ~2.2 eV. Electrochemical parameters are summarized in Table 3 and the CV graphs are shown in Figure 4.

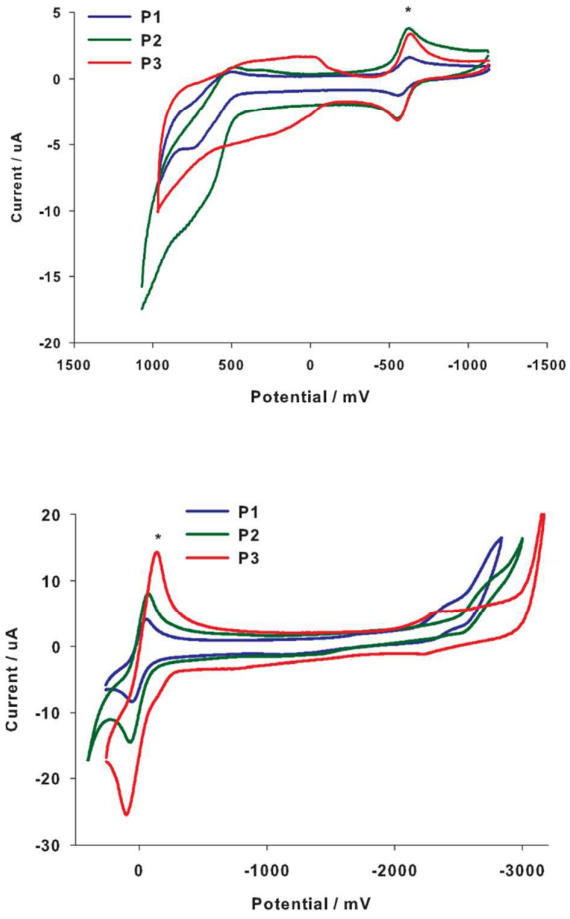

Figure 4 CV curves of polymers: Oxidation (top, in CH_2Cl_2) and reduction (bottom, in THF) with $Bu_4N^+PF_6^-$ (0.1M) as a supporting electrolyte recorded vs Fc/Fc^+ (Fc=[(η-C_5H_5)$_2$Fe] as an internal reference (marked as *) at a scan rate of 100 mV/s

Molecular Energy Levels

The HOMO and LUMO levels of the polymers were estimated experimentally by cyclic voltammetry (CV) and theoretically using density functional theory (DFT). The redox potentials are reported relative to the ferrocene/ferrocenium (Fc/Fc^+) couple at 298 K. The HOMO levels of **P1**, **P2**, and **P3** were found to be -5.29, -5.29 and -4.75 eV respectively, whereas LUMO levels of **P1**, **P2**, and **P3** were found to be -2.29 eV, -2.22 eV and -2.54 eV respectively. Confirming results from the optical characterizations, the lack of the Si-linkages in **P3** also leads to a markedly smaller HOMO-LUMO gap. In **P3** the backbone lacks the flexible Si linkage enabling more electron delocalization, and resulting in a destabilized HOMO energy

For the theoretical calculations we carried out studies on dimer models of **P2** and **P3**. Geometries were optimized using density functional theory (DFT) in the Gaussian 09 package at the DFT/B3LYP/6-31G(d,p) level.[51, 66] The HOMO-LUMO orbital plots for the dimer models for **P2** and **P3** are shown in Figure 5, together with the calculated energy levels. Confirming experimental results, silicon is disrupting the planarity and conjugation of the polymer backbone resulting in more locally confined HOMO and LUMO orbitals. The calculated HOMO and LUMO energy levels of the P2 model are found at -4.92 eV and -1.55 eV respectively, with a band gap of 3.37 eV. In P3, the molecular orbitals are much more extensive due to the effective electron conjugation without the Si-interruption. As a result, the HOMO energy is raised by ~ 0.5eV and the LUMO

energy lowered by ~ 0.4 eV, resulting in a smaller band gap. The calculated HOMO and LUMO energy levels of the P3 dimer model are -4.39 eV and -1.98 eV respectively, with a band gap of 2.41 eV. The calculated energy levels for P3 vs. P2 strongly support the experimental observations in the CV experiments

Table 3 Electrochemical Parameters of Polymers

Sample	HOMO[a] (eV)	LUMO[a] (eV)	Bandgap[a] (eV)	HOMO[b] (eV)	LUMO[b] (eV)[1]	Bandgap[b] (eV)[1]
P1	-5.29	-2.29	3.00		n.d	
P2	-5.29	-2.22	3.07	-4.92	-1.55	3.37
P3	-4.75	-2.54	2.21	-4.39	-1.98	2.41

[a] Energy levels determined by CV; [b] Energy levels determined by theoretical calculation

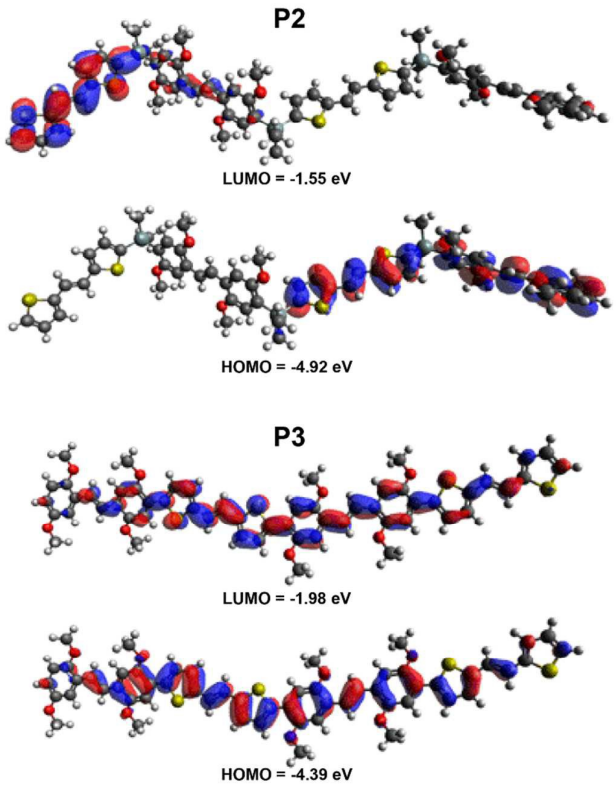

Figure 5 HOMO/LUMO orbital plots of P2 (top) and P3 (bottom) dimers, calculated by DFT at the B3LYP/6-31G(d,p) level.

Conclusions

Using ADMET, we synthesized homologous luminescent conjugated polymers with two different aromatic segments, either alternating or randomly distributed along the polymer chain, either directly connected or separated by a Si-linker. Molecular weights Mn (NMR – endgroup analysis) ranged from 4982 g/mol (**P3**), 8829 g/mol (P1) to 14600 g/mol (**P2**). The systems were studied experimentally as well as theoretically to learn about specific interactions between the aromatic units that might provide guidance for future designs. It was observed that silicon limited the π-conjugation to the defined segments, resulting in shorter wavelength emission. Random or alternating placement of the two segments did not seem to influence the absorption and emission energies much (λ_{max} at 363 nm and ~ 411 nm respectively), although **P2** with its alternating segments showed a slightly more defined absorption with slightly higher absorptivity and emission efficiency (57% vs. 51%). **P3** with alternating segments directly conjugated (without a Si-linkers) resulted in longer wavelength absorption and emission (λ_{max} at 490 nm and ~ 556 nm respectively), and slightly lower emission efficiencies (40%), most likely due to more non-radiative relaxation pathways due to the extended electron conjugation. Electrochemical measurements confirmed the optical findings and showed a smaller HOMO-LUMO bandgap for the more delocalized **P3** without Si-linkers (2.21 eV vs. 3.00-3.07 eV). DFT calculations could support the above results and analyses, as calculated model structures of **P2** also showed silicon disrupting the co-planarity and conjugation of aromatic segments, resulting in a larger HOMO-LUMO gap compared to **P3**.

Acknowledgements

This research was supported in part by a CUNY Research Foundation Grant of the PSC. The high performance computer facility used, the CUNY HPCC, is operated by the College of Staten Island and funded, in part, by grants from the City of New York, State of New York, CUNY Research Foundation, and National Science Foundation Grants CNS-0958379, CNS-0855217 and ACI 1126113. We thank Dr. Jaekle at Rutgers University for letting us perform the CV measurements in his lab.

References

1. J. Mei and Z. Bao, *Chemistry of Materials*, 2014, **26**, 604-615.
2. B. C. Thompson and J. M. Frechet, *Angew Chem Int Ed Engl*, 2008, **47**, 58-77.
3. A. C. Grimsdale, K. Leok Chan, R. E. Martin, P. G. Jokisz and A. B. Holmes, *Chemical reviews*, 2009, **109**, 897-1091.
4. J. Mei, Y. Diao, A. L. Appleton, L. Fang and Z. Bao, *J Am Chem Soc*, 2013, **135**, 6724-6746.
5. J.-T. Chen and C.-S. Hsu, *Polymer Chemistry*, 2011, **2**, 2707-2722.
6. S. A. Jenekhe and D. Zhu, *Polymer Chemistry*, 2013, **4**, 5142-5143.
7. D. M. O'Carroll, C. E. Petoukhoff, J. Kohl, B. Yu, C. M. Carter and S. Goodman, *Polymer Chemistry*, 2013, **4**, 5181-5196.
8. S. Nešpůrek, *Journal of non-crystalline solids*, 2002, **299**, 1033-1041.
9. K. Takagi, S. Kunii and Y. Yuki, *Journal of Polymer Science Part A: Polymer Chemistry*, 2005, **43**, 2119-2127.
10. H. K. Kim, M.-K. Ryu, K.-D. Kim, S.-M. Lee, S.-W. Cho and J.-W. Park, *Macromolecules*, 1998, **31**, 1114-1123.
11. G. Kwak and T. Masuda, *Macromolecules*, 2002, **35**, 4138-4142.

12. F. Wang, B. R. Kaafarani and D. Neckers, C, *Macromolecules*, 2003, **36**, 8225-8230.
13. K. Tanaka, H. Ago, T. Yamabe, M. Ishikawa and T. Ueda, *Organometallics*, 1994, **13**, 3496-3501.
14. K.-L. Liu, S.-J. Lee, I.-C. Chen, C.-P. Hsu, C.-H. Chen and T.-Y. Luh, *The Journal of Physical Chemistry C*, 2012, **117**, 64-70.
15. H. J. Brouwer, V. V. Krasnikov, A. Hilberer and G. Hadziioannou, *Advanced Materials*, 1996, **8**, 935-937.
16. S.-H. Jung, H. K. Kim, S.-H. Kim, Y. H. Kim, S. C. Jeoung and D. Kim, *Macromolecules*, 2000, **33**, 9277-9288.
17. J. Wang, J. Huang, L. Du and Z. Lan, *The Journal of Physical Chemistry A*, 2015.
18. H.-W. Wang, Y.-J. Cheng, C.-H. Chen, T.-S. Lim, W. Fann, C.-L. Lin, Y.-P. Chang, K.-C. Lin and T.-Y. Luh, *Macromolecules*, 2007, **40**, 2666-2671.
19. T.-Y. Luh and Y.-J. Cheng, *Chemical communications*, 2006, 4669-4678.
20. D.-D. H. Yang, N.-c. C. Yang, I. M. Steele, H. Li, Y.-Z. Ma and G. R. Fleming, *Journal of the American Chemical Society*, 2003, **125**, 5107-5110.
21. H. Y. Chen, J. Hou, A. E. Hayden, H. Yang, K. Houk and Y. Yang, *Advanced Materials*, 2010, **22**, 371-375.
22. Y. Tokoro, H. Yeo, K. Tanaka and Y. Chujo, *Polymer Chemistry*, 2013, **4**, 5237-5242.
23. N. Mukherjee and R. M. Peetz, *Macromolecules*, 2008, **41**, 6677-6685.
24. P. Lu, J. W. Y. Lam, J. Liu, C. K. W. Jim, W. Yuan, C. Y. K. Chan, N. Xie, Q. Hu, K. K. L. Cheuk and B. Z. Tang, *Macromolecules*, 2011, **44**, 5977-5986.
25. J. Ohshita and A. Kunai, *Acta polymerica*, 1998, **49**, 379-403.
26. Y.-J. Cheng, T.-Y. Hwu, J.-H. Hsu and T.-Y. Luh, *Chemical Communications*, 2002, DOI: 10.1039/b206308e, 1978-1979.
27. M.-C. Fang, A. Watanabe and M. Matsuda, *Macromolecules*, 1996, **29**, 6807-6813.
28. J. S. Rathore and L. V. Interrante, *Macromolecules*, 2009, **42**, 4614-4621.
29. M. Ludwiczak, M. Majchrzak, M. Bayda, B. Marciniak, M. Kubicki and B. Marciniec, *Journal of Organometallic Chemistry*, 2014, **750**, 150-161.
30. Y. J. Cheng and T. Y. Luh, *Chemistry-A European Journal*, 2004, **10**, 5361-5368.
31. N. Matsumi, T. Umeyama and Y. Chujo, *Macromolecules*, 2001, **34**, 3510-3511.
32. C. H. Yuan and R. West, *Applied organometallic chemistry*, 1994, **8**, 423-430.
33. C. H. Chen, W. H. Chen, Y. H. Liu, T. S. Lim and T. Y. Luh, *Chemistry*, 2012, **18**, 347-354.
34. M.-C. Fang, A. Watanabe and M. Matsuda, *Chemistry Letters*, 1994, 13-16.
35. R. J. Corriu, W. E. Douglas, Z.-X. Yang, F. Garnier and A. Yassar, *Journal of organometallic chemistry*, 1991, **417**, C50-C52.
36. R. J. Corriu, W. E. Douglas, Z.-x. Yang, Y. Karakus, G. H. Cross and D. Bloor, *Journal of organometallic chemistry*, 1993, **455**, 69-76.
37. J. Ohshita, D. Kanaya, T. Watanabe and M. Ishikawa, *Journal of organometallic chemistry*, 1995, **489**, 165-173.
38. W.-C. Liao, W.-H. Chen, C.-H. Chen, T.-S. Lim and T.-Y. Luh, *Macromolecules*, 2013, **46**, 1305-1311.
39. J. Ohshita, A. Matsuguchi, K. Furumori, R. F. Hong, M. Ishikawa, T. Yamanaka, T. Koike and J. Shioya, *Macromolecules*, 1992, **25**, 2134-2140.
40. S.-S. Hu and W. P. Weber, *Polymer Bulletin*, 1989, **21**, 133-140.
41. Z. Zhao, T. Jiang, Y. Guo, L. Ding, B. He, Z. Chang, J. W. Lam, J. Liu, C. Y. Chan and P. Lu, *Journal of Polymer Science Part A: Polymer Chemistry*, 2012, **50**, 2265-2274.
42. H.-W. Wang, M.-Y. Yeh, C.-H. Chen, T.-S. Lim, W. Fann and T.-Y. Luh, *Macromolecules*, 2008, **41**, 2762-2770.
43. H. R. Allcock, *Journal of Inorganic and Organometallic Polymers and Materials*, 2007, **17**, 349-359.
44. A. Sengupta, A. Doshi, F. Jäkle and R. M. Peetz, *Journal of Polymer Science Part A: Polymer Chemistry*, 2015, **53**, 1707-1718.
45. P. Atallah, K. B. Wagener and M. D. Schulz, *Macromolecules*, 2013, **46**, 4735-4741.
46. Z.-L. Li, L. Li, X.-X. Deng, L.-J. Zhang, B.-T. Dong, F.-S. Du and Z.-C. Li, *Macromolecules*, 2012, **45**, 4590-4598.
47. A. Sengupta, S. Ghosh and R. M. Peetz, *Synthetic Metals*, 2010, **160**, 2037-2040.
48. H. Mutlu, L. M. de Espinosa and M. A. Meier, *Chemical Society Reviews*, 2011, **40**, 1404-1445.
49. P. P. Matloka and K. B. Wagener, *Journal of Molecular Catalysis A: Chemical*, 2006, **257**, 89-98.
50. M. Frisch, G. Trucks, H. B. Schlegel, G. Scuseria, M. Robb, J. Cheeseman, G. Scalmani, V. Barone, B. Mennucci and G. Petersson, *Inc., Wallingford, CT*, 2009, **200**.
51. F. Wu, L. Chen, H. Wang and Y. Chen, *The Journal of Physical Chemistry C*, 2013, **117**, 9581-9589.
52. M. D. Schulz and K. B. Wagener, *Macromolecular Chemistry and Physics*, 2014, **215**, 1936-1945.
53. J. C. Speros, B. D. Paulsen, B. S. Slowinski, C. D. Frisbie and M. A. Hillmyer, *ACS Macro Letters*, 2012, **1**, 986-990.
54. B. S. Aitken, P. M. Wieruszewski, K. R. Graham, J. R. Reynolds and K. B. Wagener, *Macromolecules*, 2012, **45**, 705-712.
55. B. D. Paulsen, J. C. Speros, M. S. Claflin, M. A. Hillmyer and C. D. Frisbie, *Polymer Chemistry*, 2014, **5**, 6287-6294.
56. J. C. Speros, H. Martinez, B. D. Paulsen, S. P. White, A. D. Bonifas, P. C. Goff, C. D. Frisbie and M. A. Hillmyer, *Macromolecules*, 2013, **46**, 5184-5194.
57. I. F. Perepichka, D. F. Perepichka, H. Meng and F. Wudl, *Advanced Materials*, 2005, **17**, 2281-2306.
58. F. Babudri, A. Cardone, T. Cassano, G. M. Farinola, F. Naso and R. Tommasi, *Journal of Organometallic Chemistry*, 2008, **693**, 2631-2636.
59. N. Blouin, A. Michaud, D. Gendron, S. Wakim, E. Blair, R. Neagu-Plesu, M. Belletete, G. Durocher, Y. Tao and M. Leclerc, *Journal of the American Chemical Society*, 2008, **130**, 732-742.
60. H. K. Kim, M.-K. Ryu and S.-M. Lee, *Macromolecules*, 1997, **30**, 1236-1239.
61. C. B. Nielsen and I. McCulloch, *Progress in Polymer Science*, 2013, **38**, 2053-2069.
62. T. A. Tan, T. M. Clarke, D. James, J. R. Durrant, J. M. White and K. P. Ghiggino, *Polymer Chemistry*, 2013, **4**, 5305-5309.
63. K. L. Opper and K. B. Wagener, *Journal of Polymer Science Part A: Polymer Chemistry*, 2011, **49**, 821-831.
64. H. Weychardt and H. Plenio, *Organometallics*, 2008, **27**, 1479-1485.
65. K. Mahmood, H. Lu, Z.-P. Liu, C. Li, Z. Lu, X. Liu, T. Fang, Q. Peng, G. Li and L. Li, *Polymer Chemistry*, 2014, **5**, 5037-5045.
66. B. C. Popere, A. M. Della Pelle, A. Poe, G. Balaji and S. Thayumanavan, *Chemical Science*, 2012, **3**, 3093.
67. A. Sengupta, A PhD Dissertation, *City University of New York*, 2012.

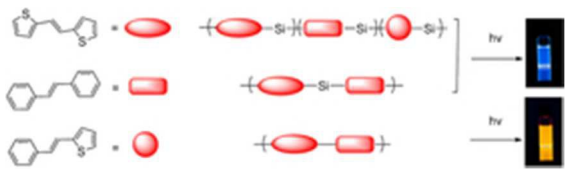

23x6mm (300 x 300 DPI)